Chapter 2

Concepts and Techniques

In this chapter we will briefly discuss some of the basic concepts that are of general relevance for the following. Further details and definitions are given as they are needed in the respective sections.

2.1 Digital Images

The primary data type we will have to deal with in this work are two- and three-dimensional images. A continuous image is a scalar valued function

$$I_{2D} : D_{2D} \subset \Re^2 \to \Re, \qquad I_{3D} : D_{3D} \subset \Re^3 \to \Re$$

In the remainder of this section we will limit the discussion to two-dimensional images, since the three-dimensional case is completely analogous.

The domains of images given in computer vision are almost always rectangular regions:

$$D = [x_0 \dots x_1] \times [y_0 \dots y_1]$$

A digital image is a discrete approximation of the continuous function. It is given as a set of function values defined on a grid. The grid is typically a rectangular hexahedral grid, often with uniform grid spacing.

$$\begin{aligned} \hat{D} = \{(x_i, y_j) \in \Re^2 | \quad & x_i = x_0 + i\Delta_x, \quad i = 0 \dots N_x - 1 \\ & y_i = y_0 + j\Delta_y, \quad j = 0 \dots N_y - 1\}. \end{aligned} \tag{2.1}$$

In order to formulate algorithms that process digital images, a proper interpolation method has to be chosen. A frequently used interpolation scheme is the piecewise constant interpolation, where the image looks like a regular assembly of little square tiles (cf. 2.1). These are called *pixels*, which is short for picture elements, or *voxels* for volume elements in the three dimensional case. The common use of piecewise constant interpolation leads to a common overlooking of the real nature of a digital image. Alvy Ray Smith fights against this misinterpretation in his article *A Pixel*

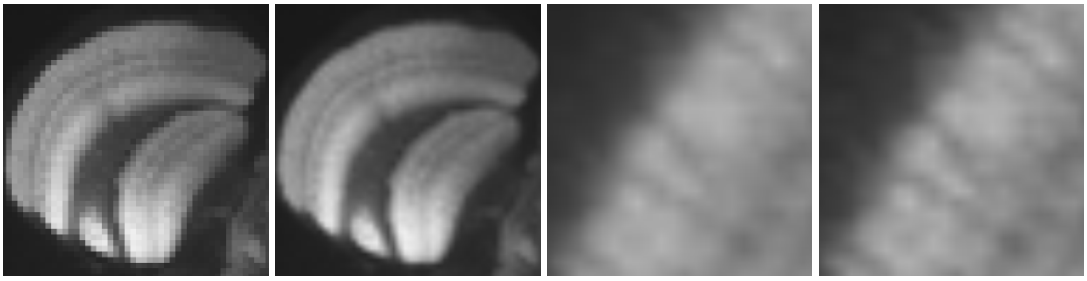

Figure 2.1: Comparison of different interpolation schemes in a digital image (at low resolution for demonstration purpose). The first image uses piecewise constant interpolation. The second image shows the same data set with bi-linear interpolation. The image looks much smoother and more natural. On the other hand the visual information about the sampling resolution is lost: It is not distinguishable whether the blur stems from the smoothness of the continuous signal or the low sampling frequency. The two right images are close-ups of slices that have been extracted from the three dimensional data set in a direction not orthogonal to one of the major axis. While for the left of the two images tri-linear interpolation was used, the right data set uses an approximation of the sinc-function as filter kernel. The difference may be harder to see in the printed version than in the online document, but in the right image some of the details are preserved noticeably better than in the left one.

is Not *a Little Square, ...* [119], which is worth reading as an introduction to this subject. In the following, however, it will become clear in which cases it makes sense to display pixels as little squares and that sometimes for a user a pixel indeed *is* a little square.

Instead of the grid point in the digital image domain or the sample value at that point, the term pixel (voxel) is often used to refer to the rectangular (cuboidic) region that is composed by all points nearest to such a grid point, i.e. the cell of the dual grid. This is the definition that we prefer. The grid point is referred to as the *center of the pixel*. The image value at a location within such a pixel is determined by the interpolation scheme.

Beside constant interpolation, one of the most commonly used interpolation scheme is (tri-)linear interpolation. The image value at a location $\vec{p} = (p_x, p_y)$ is computed as follows: Let (i, j) be given such that

$$x_i \leq p_x < x_{i+1}, \quad y_j \leq p_y < y_{j+1}$$

Let $\vec{u}$ be the relative location within the grid cell:

$$u_x = \frac{p_x - x_i}{x_{i+1} - x_i}, \quad u_y = \frac{p_y - y_i}{y_{i+1} - y_i}.$$

Then the interpolated value is given by

$$\begin{aligned} I_{\text{lin}}(\vec{p}) = (1 - u_y) \quad & ((1 - u_x)I(x_i, y_j) + u_x I(x_{i+1}, y_j)) + \\ u_y \quad & ((1 - u_x)I(x_i, y_{j+1}) + u_x I(x_{i+1}, y_{j+1}))\,. \end{aligned} \tag{2.2}$$

In Figure 2.1 we can see that linear interpolation leads to a smoother and more natural appearance of the images. However, it also hides resolution information, therefore it has to be carefully decided when to use it. Details are given in the figure caption. Note that the efficient use of an interpolation scheme for display purpose requires consideration of the output device resolution.

If we recall the initial definition of a continuous image and the interpretation of a digital image as a sampling of that continuous function, a different interpolation scheme can be derived. According to the Nyquist sampling theorem, a continuous function can be fully reconstructed from a discrete sampling if the sampling frequency is at least twice the largest frequency occuring in the signal. If a lower sampling frequency is chosen, aliasing artifacts can occur [102]. With the assumption that the continuous function represented by a digital image was band-limited in this way, this function could be reconstructed from the samples and evaluated exactly. For the one-dimensional case and if $x_0 = 0$ this is done with:

$$I_{\text{recon}}(x) = \Delta_x \sum_{i=0}^{N_x-1} I(x_i) \frac{sin\,(2\pi(x - i\Delta_x)/(2\Delta_x))}{\pi(x - i\Delta_x)} \tag{2.3}$$

We can see that Equation (2.3) is essentially a discrete convolution with the *sinc* function $sin(x)/x$. This function has infinite support but its value is bounded by $1/x$. Therefore, it can be reasonably approximated with a finite filter kernel. This leads to interpolation schemes which are slower but more accurate than linear interpolation. Results are shown in Figure 2.1. Note that the subtle differences can be seen better in the electronic version of this paper than in the printed version.

2.2 Data Acquisition

A complete description of three dimensional image acquisition techniques is not in the scope of this work. We will limit ourselves to mention the most relevant types for our work and the specific properties of corresponding data sets.

The most important acquisition technique for this work is confocal laser scanning microscopy (LSM) [115]. If a thick specimen is put under a conventional light microscope it is possible to focus to different depths. Nevertheless, light from the out-of-focus planes will enter the detectors. A confocal microscope has additional pin-holes which avoid this. Only light from one specific point can enter the eye. In addition, a laser excites only a small region in the specimen. The principle of an LSM is explained in figure 2.2. The optical resolution in the axial (z) direction is not the same as the lateral one. Depending on the numerical aperture of the used objective it is at least 2 to 5 times lower in axial direction. This effect complicates the data treatment significantly.

Another practical problem is due to the relationship of an objective's resolution and the field-of-view. The better the resolution is, the smaller is the part that can be recorded. In lateral direction this limitation can partly be overcome by mechanically shifting the specimen with a motor-stage, record several bricks and later assemble the mosaic to one large data set.

An LSM recording requires that the recorded tissue is fluorescent, i.e. that light is emitted when the tissue is excited with a laser. Since in general this is not the case the specimen has to undergo a staining procedure. For studying the anatomy of insect brains it was desirable to develop a histological procedure which uniformly labels the neuropil of a complete brain, which is not trivial, since whole brains are relatively thick. K. Rein has developed a specific two-antibody method [105]: The primary antibody ($nc82$) recognizes a specific antigen in the fly brain, the second is conjugated with a fluorescent dye and recognizes the first antibody. Details are given in [105]. A similar procedure is used by R. Brandt for honey bees.

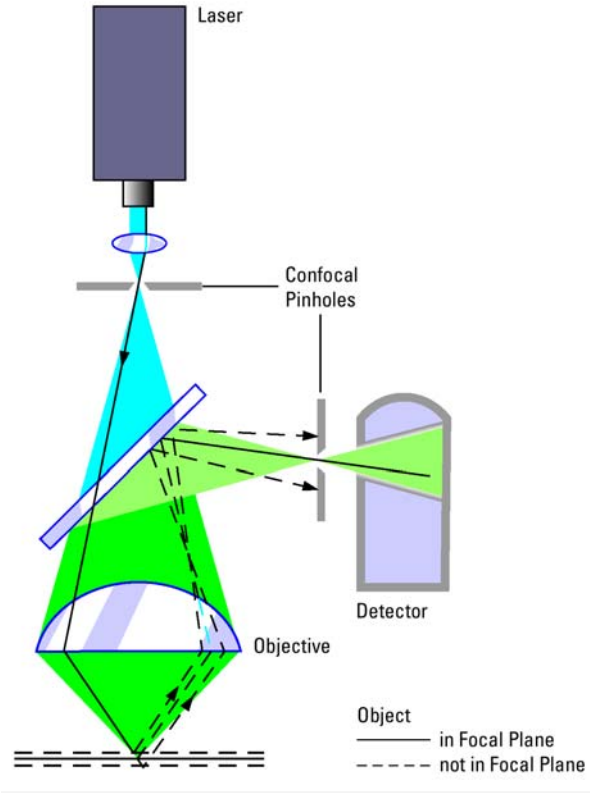

Figure 2.2: Principle of a confocal microscope: Due to a pinhole the exciting laser illuminates only a small part of the specimen. A pinhole in front of the detectors assures that only light from one specific point reaches the detector. The point of excitation and the point of detection coincide; they lie in the same focal plane, they are *confocal*. The microscope is steered by a computer that scans the entire specimen in x,y, and z direction. Image modified from Leica [87].

This way structures formed by the neuropil-tissue can be imaged. Here neuron cells are not resolved individually. Especially in the honeybee brain it is also possible to individually identify and record some of the bigger neuron cells: In an experimentally demanding procedure an electrode is introduced into the cells' primary neurit in a living individual. The electrode can be used to measure the animals response to stimuli. Then a fluorescent dye is injected into the neuron, and after preparation the morphology of the neuron can be recorded.

A general problem with fluorescent dyes is bleaching. The intensity of the exiting laser light destroys the dye molecules. Therefore, only a very limited exposure time can be used. This often leads to a very low signal-to-noise ratio, especially in regions of thin structures with small dye concentration.

Three dimensional image volumes can also be recorded with conventional light microscopes, by shifting the focus plane through the specimen, e.g. with a motorized z-stage. The out-of-focus

light that blurs the image can then partially be removed using deconvolution algorithms [46].

Deconvolution tries to inverse the error introduced by the imaging process. The error can be modeled as a convolution of the original object's signal with the microscopes transfer function, the so called point-spread-function. Under certain conditions Deconvolution can also be used in confocal microscopy to increase the resolution of the recorded images. For further details of deconvolution we refer to [45, 129].

Other important techniques for this work are computer tomography (CT) and magnetic resonance imaging (MRI) [68]. The spatial resolution of these methods is not yet good enough for them to be used for insect brain anatomy, but they are standard techniques for vertebrate brain research and some first experiments with MRI imaging insect brains have been undertaken.